Direct Measurements of Lightning-Induced Coupling to a Spacecraft Umbilical Cable

Dr. Dustin Hill[a] and Dr. Carlos Mata[a]
[a]Scientific Lightning Solutions, LLC, Merritt Island, FL, USA

Abstract

Lightning-induced currents and voltages were directly measured on a legacy spacecraft umbilical cable installed at the Kennedy Space Center in Florida. Measurements were recorded for 88 return strokes that terminated within 3km of the umbilical instrumentation during 2022 and 2023. Overall umbilical current, inner shield current, and inner twisted-shielded pair (TSP) conductor current were simultaneously measured in addition to TSP pin voltages. The umbilical current peaks were found to be well correlated with the current peaks of the S12 inner shield, while the peaks of the umbilical current derivative and the S12 inner shield current derivative were found to be strongly correlated with the TSP voltage peaks. Finally, the S12 inner shield current peaks were found to be strongly correlated with the short-circuit current on the TSP conductor. Correlations were established via simple second order polynomial or linear functions. Simultaneous current measurements demonstrated the effectiveness of multi-layer shielding toplogies where the current amplitude and risetime were reduced from overall umbilical current, to S12 inner shield current, to TSP conductor current.

1 Introduction

Lightning poses a significant challenge for space launch operations, particularly at the Kennedy Space Center (KSC) and Cape Canaveral Space Force Station (CCSFS) in Florida, where both the lightning ground flash density [1] and the launch cadence are high. KSC/CCSFS supported a total of 73 orbital launches in 2023, or a launch about every 5 days. Spacecraft, launch vehicles, and associated ground support equipment (GSE) are susceptible to the direct and indirect effects of lightning during integration, transport to the launch facility, pre-launch check-outs and testing, and day-of-launch operations. Spacecraft and launch vehicles are connected to GSE via large, complex cables referred to as “umbilicals". Umbilical cables typically incorporate high-density connectors to carry a multitude of signals for communication, control, and monitoring circuits. The umbilical cables are typically constructed with multiple shielding layers composed of overbraids and metallic tapes, which cover internal twisted-shielded cable pairs. During past operations, the tranceivers, level-shifters, and other critical electronics on both the spacecraft and GSE sides of the umbilical cables have experienced damage due to coupled lightning transient signals. *In situ* measurements were not available to quantify the amplitudes, energy content, and waveform characteristics of these damaging events in order to determine how manufacturer-specified component thresholds had been exceeded. Such lighting-related damage requires expensive and time-consuming retest operations. Further, the potential for on-orbit manifestation of latent damage exists where components were stressed (but not to failure) during pre-launch exposure to lightning.

For some missions (particularly NASA science initiatives), lightning transient monitoring systems are utilized to provide direct measurements of the overall umbilical current in addition to electromagnetic fields near the spacecraft. Engineers utilize the overall umbilical current data along with modeled cable transfer impedances to estimate the coupled pin voltages on the inner conductors. Many times, the use of lightning transient monitoring systems is not feasible due to cost, schedule, and installation restrictions at the launch site.

Prior to Summer 2022, NASA LSP engineers conducted tests on the the response of a legacy spacecraft umbilical cable to various electromagnetic excitation sources produced inside an anechoic chamber at CCSFS. Note that laboratory excitation sources, while valuable from a repeatability standpoint, cannot accurately replicate signals radiated by real lightning. Further *in situ* evaluation of pin-to-pin voltages for a spacecraft umbilical cable were also described in [5], where an impulse generator was utilized to provided “lightning-like" excitation. Based on known challenges and laboratory data collection, Scientific Lightning Solutions, LLC was tasked by the NASA Launch Services Program (LSP) to conduct a field study to directly monitor the coupling of radiated actual lightning signals to a legacy spacecraft umbilical cable. The following study goals were established:

- Measure lightning-induced currents on the umbilical cable (both overall and on the inner conductors/shields).
- Measure lightning-induced single-ended and differential voltages on the umbilical cable twisted shielded pairs.
- Develop equations to predict the induced currents/voltages on the inner conductors based on the

overall umbilical current measurements.

The study period spanned the latter portions of Summer 2022 and Summer 2023.

2 Instrumentation

The umbilical instrumentation system was installed at the northern end of Static Test Road at Camera Site 15, KSC. An aerial image illustrating the location of the umbilical instrumentation system is shown in Figure 1. The umbilical cable is about 50-ft in total length and was elevated about 6-ft off the ground on wooden supports (see Figure 2). The umbilical cable has a high-density rectangular connector at the launch vehicle interface and three individual high-density circular connectors at the opposite end for connections to GSE. For the field installation, the launch vehicle interface connector was mated to the shielded enclosure containing the data acquisition hardware (see foreground of Figure 2) and the three circular connectors were located at the field end of the cable. Connector 'P1' at the field side of the cable was mated to a smaller aluminum enclosure. Terminal blocks are mounted inside the field enclosure that allow the inner conductors of the harness, which are broken out in pigtails, to be connected in various configurations. Connector 'P1' contains twisted shielded pairs being monitored (TSP1, TSP2, TSP3, and TSP4). The pinouts for the field end of cable (P1) and the instrumentation end of the cable (PU2) are shown in Figure 3. Note that shield connections 'S12', 'S5', and 'S34' are all independent and were confirmed to be electrically isolated. The shields within group 'S' are all electrically connected and were confirmed to be electrically isolated from 'S12', 'S5', and 'S34'. Note that 'S12' is the inner shield for TSP1 and TSP2 and 'S34' is the inner shield for TSP3 and TSP4.

A roughly 50-ft section of 1-in tubular stainless steel braided wire was bonded to the instrumentation enclosure and then routed along the ground under the elevated umbilical cable to the aluminum enclosure on the field end of the cable. The braided wire was similarly bonded to the field enclosure, completing the loop. The total enclosed loop area formed by the umbilical cable and the ground connection is about 300-sqft. Note this loop area simulates the ground loop formed when an umbilical cable is mated to the grounded spacecraft.

Lightning data were acquired via two of SLS' Jupiter Transient Monitoring System (TMS) high-speed data acquisition systems. The Jupiter TMS that supported the umbilical instrumentation provided continuous, event-driven data collection. Each system supports four independent, differential analog input channels that are sampled at 80 MS/s (12.5 ns sampling resolution) with about 40 MHz of analog bandwidth. Jupiter TMS is a true zero-deadtime data acquisition system, that is, it is capable of triggering continuously without missing a single sample of data. This unique capability is critical for ensuring data are recorded for 100% of lightning events that occur within the defined area of interest. Each Jupiter TMS unit was provided with a GPS timing source, which allows captured events to be correlated with sample-point accuracy, and allows accurate correlations with data from large-scale lightning lo-

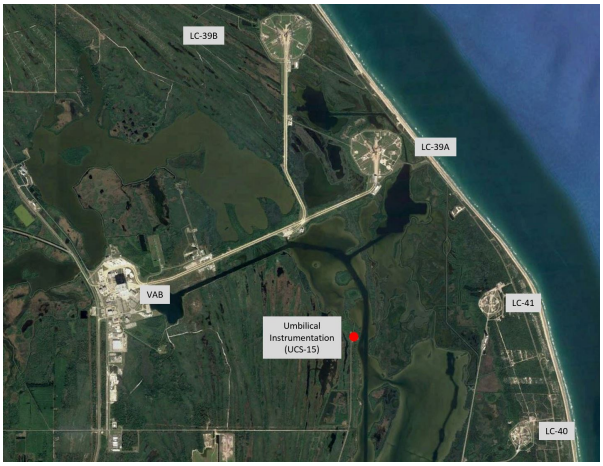

Figure 1 2023 umbilical instrumentation installation at Camera Site 15 and KSC.

Figure 2 Image of the umbilical cable. The instrumentation enclosure containing the Jupiter TMS transient recorders is shown in the foreground.

Pinout		
	PU2	P1
TSP1	180	R
	185	Y
TSP2	176	F
	181	K
S12	187	X
S5		Q
TSP3	12	H
	17	O
TSP4	16	W
	21	d
S34	9	P
S	41	
	49	
	157	
	167	
	169	

Figure 3 Connector pinouts for the four TSPs and associated cable shields for the NASA umbilical cable. P1 connections correspond to the field end of the cable and PU2 connections correspond to the instrumentation end of the cable.

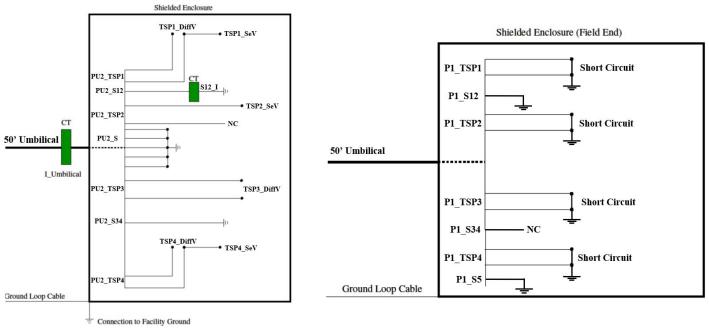

Figure 4 Schematic representation of the umbilical instrumentation system from June 25-August 2, 2022. The ground loop cable that connects the instrumentation and field enclosures is shown.

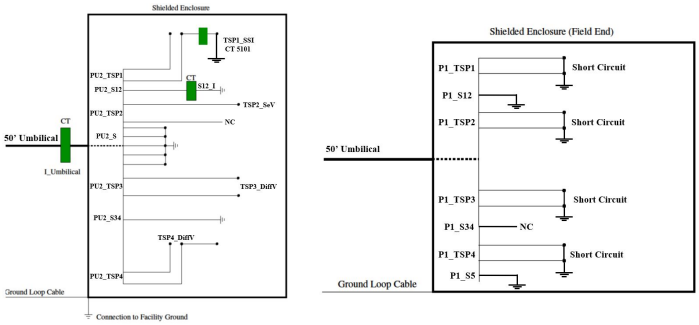

Figure 5 Schematic representation of the umbilical instrumentation system from August 3-September 14, 2022. The ground loop cable that connects the instrumentation and field enclosures is shown.

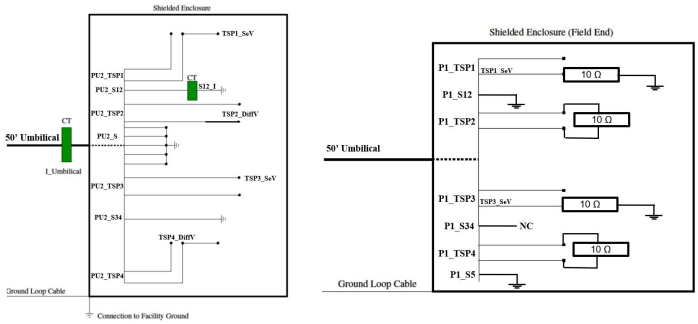

Figure 6 Schematic representation of the umbilical instrumentation system from July 12-September 17, 2023. The ground loop cable that connects the instrumentation and field enclosures is shown.

cation systems. When a pre-defined trigger threshold is exceeded on any of the four channels, Jupiter TMS stores the four-channel data into permanent memory and immediately pushes the data file to a remote cloud server. Trigger levels, polarity, and logic are independently configured for each data acquisition channel. In addition, the input dynamic range of each channel was independently adjusted to maximize the resolution of the acquired data. Channel input impedances were configured at either 50Ω (for current measurements) or 1MΩ (for voltage measurements). Pearson current transformers were utilized to measure the overall umbilical current (Model 5949), the S12 inner shield current (Model 4100), and the TSP1 short-circuit current (Model 5101).

The instrumentation systems are fully solar-powered and communicate data and status to a remote cloud server via a cellular modem connection. Operation is continuous with sufficient battery backup capacity to maintain the instrumentation for 2-3 days, even during cloudy conditions.

Three configurations of the umbilical cable were utilized during the study, spanning June 25-August 2, 2022 (Figure 4), August 3-September 14, 2022 (Figure 5), and July 12-September 17, 2023 (Figure 6). The schematic representations of the umbilical cable connections depict the measurements at left and field terminations shown at right. The ground loop cable that connects the instrumentation and field enclosures is shown.

3 Data Summary

SLS obtained lightning strike location data from the NLDN (National Lightning Detection Network), operated by Vaisala, and MERLIN (Mesoscale Eastern Range Light-

ning Information Network), operated by the 45th Weather Squadron, for 2022 and 2023, respectively. During 2022, SLS was provided access to the NLDN cloud-to-ground lightning database. This access was not available during 2023. NLDN and MERLIN provide a typical strike location accuracy of about 100-150m for strikes to ground at KSC/CCSFS [2][3]. Data obtained from the umbilical instrumentation system were correlated against the NLDN/MERLIN return stroke time-stamps for strokes reported with peak currents larger than 10kA (either positive or negative polarity). A threshold of 10kA was chosen based on prior analyses and published literature to statistically exclude misreported cloud-to-cloud lightning events [4]. Further, only events recorded on the umbilical instrumentation system with overall induced currents greater than 1A were considered. A total of 88 return strokes reported by NLDN/MERLIN with peak current larger than ±10kA and within 3km of the instrumentation were recorded during the study period.

4 Analysis

The primary goal of the present study was to develop equations to relate the measured currents on the overall umbilical cable to the currents and voltages coupled to the inner conductors/shields. These equations can be utilized when a comprehensive set of measurements is not available, which is the case for most orbital launches. In some prior operational installations, the overall umbilical current is directly measured, but currents and voltages on the inner conductors are not.

4.1 Overall Umbilical Current Vs. S12 Inner Shield Current

The current peaks for the overall umbilical current and S12 inner shield current were measured for 88 common events in 2022 and 2023. Note the configuration of the overall umbilical current and S12 inner shield current measurements did not change throughout the study. A scatter plot showing the current peaks for common events is shown in Figure 7 with overall umbilical current peak on the horizontal axis and S12 inner shield current peak on the vertical axis. A second order polynomial function provided the best fit to the distribution using the bisquare weights method (see Equation 1). The best fit curve is shown in red ($n = 88$, $RSS = 0.893$, $R^2 = 0.933$). Data points at higher overall umbilical current amplitudes tended to diverge further from the best fit curve.

$$S12_I = 0.00251 \cdot I_{Umb}^2 + 0.06862 \cdot I_{Umb} + 0.06658 \quad (1)$$

An example waveform plot of the overall umbilical current (left axis) and the S12 inner shield current (right axis) is shown in Figure 8 for a negative cloud-to-ground stroke on July 18, 2022 at 22:06:35.008 (UT). NLDN reported the stroke a distance of 642m from the instrumentation with peak current of about -73kA. Note this was an unusually strong negative subsequent stroke. The stroke was preceded by a dart-stepped leader with regularly spaced leader

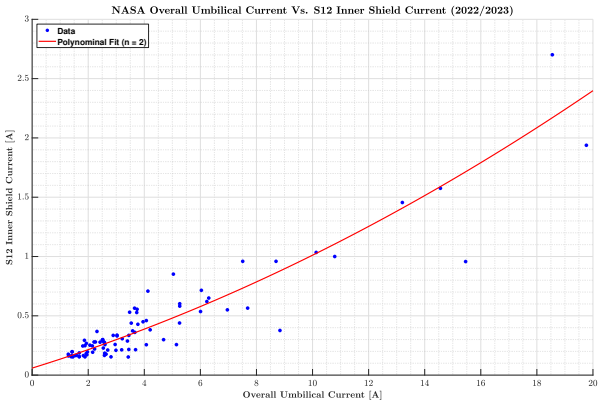

Figure 7 Scatter plot of the overall umbilical current peaks vs. S12 inner shield current peaks for 2022/2023 (n = 88 events).

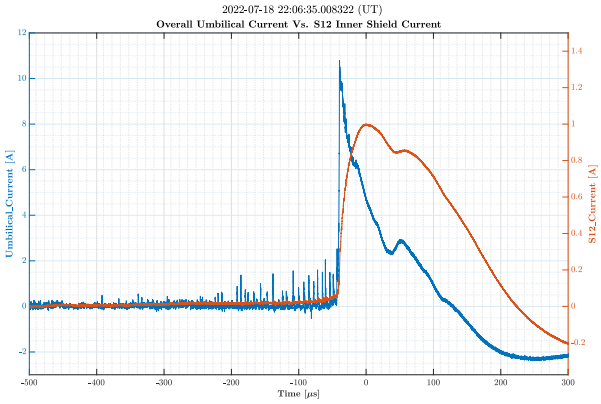

Figure 8 Example waveforms for the overall umbilical current (left) vs. S12 inner shield current (right) for an event on July 18, 2022 at 22:06:35.008 (UT).

step pulses evident in the overall umbilical current waveform in the several hundred microseconds prior to the return stroke. The overall umbilical current peak was about 10.8A. The S12 inner shield current exhibited a slow rise beginning about 400μs prior to the return stroke. The S12 inner shield current peaked about 37μs after the overall umbilical current at a level of about 1A. The S12 inner shield current has a longer pulse-width than the overall umbilical current with a slower decay.

4.2 Overall Umbilical Current Derivative Vs. TSP1 Single-Ended Voltage

The overall umbilical current peaks were poorly correlated to the TSP1 single-ended voltage peaks. Based on the raw waveform data, the shape of the TSP1 single-ended voltage measurements demonstrates a strong resemblance to electric/magnetic field derivative waveforms recorded in close proximity to the umbilical instrumentation systems. How does the overall umbilical current derivative waveform peak correlate to the TSP1 single-ended voltage peak? In order to perform this correlation, the first step involved computing the numerical derivative of the overall umbilical current waveform. Numerical differentiation is an inherently noisy process. Multiple signal processing

techniques were tested to produce the numerical derivative with the maximum signal-to-noise ratio. The best solution was to apply a Savitzky-Golay polynomial smoothing filter to the raw umbilical current data before taking the numerical derivative. Optimal filter parameters were polynomial order of 5 and frame length of 25. The Savitzky-Golay filtering technique successfully preserves the high-frequency components of the input signal while still adequately rejecting noise. After the numerical differentiation was performed, the peak numerical derivatives for each waveform were tabulated. A scatter plot of the overall umbilical current derivative peaks plotted against the TSP1 single-ended voltage peaks is shown in Figure 9 (n = 69 events) for 2022 data. There were only 16 events captured in 2023, which does not provide a statistically significant sample. The linear best fit curve is shown in red and is represented by Equation 2. Curve fit parameters were $n = 69$, $RSS = 0.265$ and, and $R^2 = 0.845$, indicating a quite strong correlation.

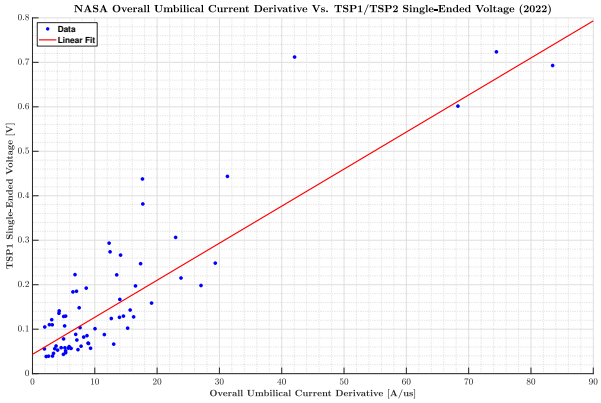

Figure 9 Scatter plot of the overall umbilical current derivative peaks vs. TSP1/TSP2 single-ended voltage peaks for 2022 (n = 69 events).

$$TSP1_{SEV} = 0.008331 \cdot \frac{dI_{Umb}}{dt} + 0.04345 \qquad (2)$$

4.3 S12 Inner Shield Current Derivative Vs. TSP1 Single-Ended Voltage

The correlation between the S12 inner shield current peaks and the TSP1 single-ended voltage peaks was similarly weak to the comparison to the overall umbilical current peaks. A similar topology was followed to take the numerical derivative of the measured S12 inner shield current waveforms and compare the peak derivatives to the TSP1/TSP2 single-ended voltage peaks. The Savitzky-Golay smoothing method was utilized with polynomial order of 5 and frame length of 25. Note there were a total of 26 events during 2022 where the S12 inner shield current derivative was well resolved. A scatter plot of the S12 inner shield current derivative peaks plotted against the TSP1/TSP2 single-ended voltage peaks is shown in Figure 10. The relationship was best fit with a second order polynomial function according to Equation 3. Curve fit parameters were $n = 26$,$RSS = 0.019$, and $R^2 = 0.978$, indicating a very strong correlation. The S12 inner shield current derivatives peaks were better correlated (with lower residuals) to the measured TSP1/TSP2 single-ended voltage peaks than the overall umbilical current derivative peaks.

$$TSP1_{SEV} = 1.492 \cdot \frac{dS12_I^2}{dt} + 1.128 \cdot \frac{dS12_I}{dt} - 0.0009491 \qquad (3)$$

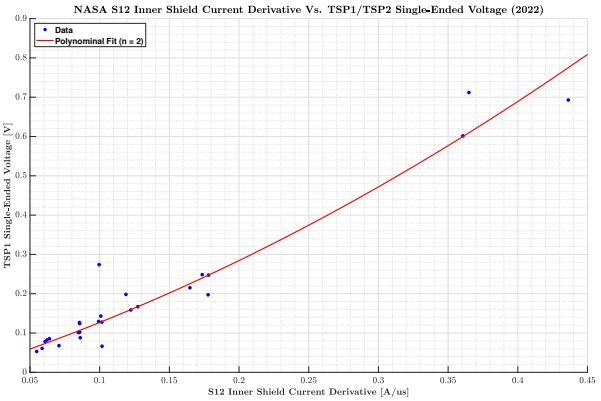

Figure 10 Scatter plot of the S12 inner shield current derivative peaks vs. TSP1 single-ended voltage peaks for 2022 (n = 26 events).

4.4 Overall Umbilical Current & S12 Inner Shield Current Vs. TSP1 Short-Circuit Current

The short-circuit current for TSP1 was measured for 24 events from August 8-17, 2022. The measured peaks of the TSP1 short-circuit current were correlated against the measured peaks of both the overall umbilical current and S12 inner shield current. This set of measurements presents a very unique opportunity to analyze currents recorded at three different “depths" within a single umbilical cable. Example waveforms for a first stroke negative polarity event on August 13, 2022 at 19:20:12.420 (UT) are shown in Figure 11. The overall umbilical current, S12 inner shield current, and TSP1 short-circuit current are shown in blue, orange, and black, respectively. NLDN reported the stroke 163m from the instrumentation with peak current of -19.3kA. As with prior examples, the overall umbilical current exhibits a relatively strong response to the leader step pulses in the hundreds of microseconds prior to the return stroke as the leader channels descend towards ground level. The overall umbilical current peaked at about 7.7A. The S12 inner shield current exhibits the typical slower rise-time than the overall umbilical current and peaks about 32μs after the overall umbilical current at about 0.56A. The high-frequency fluctuations associated with the leader step pulses are not pronounced on the S12 inner shield current measurements. The TSP1 short-circuit current rises significantly slower than the S12 inner shield current and peaks about 48μs after the S12 inner shield current (nearly 80μs after the overall umbilical current) at a level of about 0.33A. The decay after the current peak is slowest for the TSP1 short-circuit current measurements. These example waveforms clearly illustrate the reduction in both in-

duced current amplitude and high-frequency content from a multi-layer shielding topology.

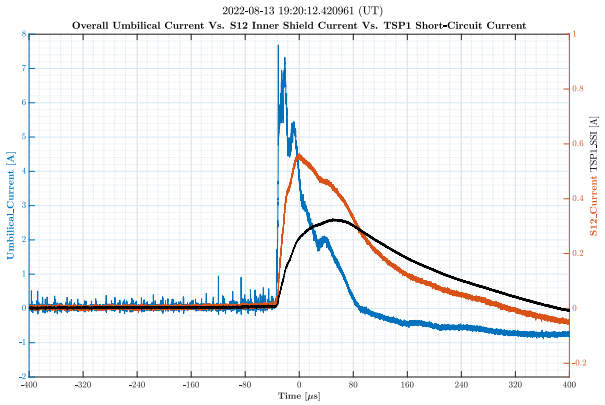

Figure 11 Waveforms for the overall umbilical current (blue, fastest risetime), S12 inner shield current (orange, slower risetime), and TSP1 short-circuit current (black, slowest risetime) associated with a negative polarity first return stroke on August 13, 2022 at 19:20:12.420 (UT). The S12 and TSP1 current amplitudes correspond to the right axis and the overall umbilical current amplitude corresponds to the left axis.

A second order polynomial best fit curve was established for the relationship between the S12 inner shield current and TSP1 short-circuit current peaks (see Figure 12) according to Equation 4. Curve fit parameters were $n = 22$, $RSS = 0.005$, and $R^2 = 0.977$, indicating a very strong correlation.

$$TSP1_{SSI} = -0.1346 \cdot S12_I^2 + 0.7368 \cdot S12_I - 0.01178 \quad (4)$$

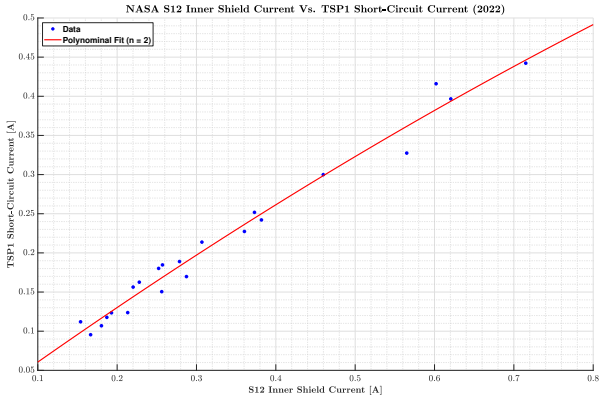

Figure 12 Scatter plot of the S12 inner shield current peaks vs. TSP1 short-circuit current peaks for 2022 (n = 22 events).

5 Conclusions

The analyses performed for 2022/2023 data demonstrated that measurements of the overall umbilical current and/or it's derivative can be used to help predict currents and voltages on the inner conductors of large umbilical cables. These relationships were generally best fit with second order polynomial or linear functions. The induced voltages on the internal conductors strongly resemble the waveshapes of the overall current derivative and inner shield current derivative. These observations have important implications on how spacecraft umbilical cables are instrumented in the operational environment.

Based on the volume of data analyzed, it is clear that the umbilical current derivative rather than the umbilical current is a more valuable measurement for predicting induced currents and voltages peaks on the inner shields and conductors. Numerical differentiation (an inherently noisy and challenging technique) was utilized to extract the current derivative from the experimental current data. This approach, while functional to demonstrate the observed relationships, may not fully reproduce the waveshape and high-frequency content of a directly measured current derivative signal. Future experimental efforts to predict coupling to the inner conductors and shields of umbilical cables should incorporate direct current derivative measurements in addition to overall current measurements. This recommendation also extends to the operational environment. The overall umbilical current is also a valuable measurement, particularly for quantifying the overall energy coupled into the umbilical cable.

Finally, the experimental results for umbilical data clearly show the benefits of multi-layer shielding topologies by reducing both induced current amplitudes and high-frequency content on inner conductors from actual lightning-induced coupling. To the authors' knowledge, these unique measurements are the first of their kind on a spacecraft umbilical cable tested to real lightning stimuli outside the laboratory.

6 Literature

[1] Roeder, W.: A New Lightning Climatology for Cape Canaveral Air Force Station and NASA Kennedy Space Center: AMS, 2017.

[2] Hill, J.D.: Mata, C.T.: MERLIN Low Detection Efficiency Study Results: First Two Years, International Conference on Lightning Protection, Cape Town, 2022.

[3] Hill, J.D.: Mata, C.T.: Close Observations of Forked and Upward-Illumination Return Strokes at the Kennedy Space Center/Cape Canaveral Air Force Station, International Conference on Lightning Protection, Estoril, 2016.

[4] Murphy, M. J.: J. A. Cramer: R. K. Said: Recent History of Upgrades to the U.S. National Lightning Detection Network. J. Atmos. Oceanic Technol., 38, 573–585, 2021.

[5] Trout,D.:Edwards,P.:Tracz,J:Gonzales,G: Shield to Pin Coupling of Lightning-Like Transients on Payload Umbilical Cables on a Launch Pad. IEEE Aerospace Conference, Big Sky, MT, USA, 2020.

Dr. Hill received his Ph.D. degree in Electrical Engineering from the University of Florida. His research at the ICLRT focused on the mechanisms and physics of natural and triggered lightning leader propagation and ground attachment, including the related high-energy physics. Dr. Hill has authored or co-authored more than 60 articles in peer-reviewed journals, more than 45 conference publications, and more than 50 technical reports. Dr. Hill spent four years working in Kennedy Space Center's Advanced Electronics and Technology Development Laboratory, where he specialized in the design and implementation of robust, highly-accurate lightning location systems, custom lightning monitoring systems, high-speed photographic and biological imaging systems, and electromagnetic sensors. He is now a Lightning Subject Matter Expert at Scientific Lightning Solutions, where he specializes in the design of state-of-the-art lightning instrumentation systems, design and testing of complex lightning protection systems, lightning damage mitigation, and standards compliance. Dr. Hill has extensive experience in custom software development with emphasis on lightning waveform and image analysis.

Dr. Mata received his Ph.D degree in Electrical Engineering from the University of Florida. He was the lightning subject matter expert and technical lead of Kennedy Space Center's Advanced Electronics and Technology Development Laboratory for 12 years. He directed the program that designed the lightning protection and lightning instrumentation systems for NASA's Launch Complex 39B, perhaps the most sophisticated lightning protection and monitoring system in the world. Dr. Mata is the recipient of many awards, including NASA's Distinguished Public Service Medal and the NASA KSC Engineer/Scientist of the Year Award. Dr. Mata has also worked extensively with the International Center for Lightning Research and Technology (ICLRT) to evaluate and refine lightning instrumentation systems used to monitor high-tech vehicles, payloads, and high-value assets at the Kennedy Space Center, Cape Canaveral Air Force Base, and other Department of Defense locations.